Limitations of Craniocaudal Thallium-201 and Technetium-99m-Sestamibi Mammoscintigraphy

A.H. Maurer, D.F. Caroline, F.J. Jadali, T.A. Manzone, W.P. Maier, F.C. Au and S.F. Schnall

Division of Nuclear Medicine, Department of Diagnostic Imaging and the Departments of Surgery and Medical Oncology, Temple University Hospital, Philadelphia, Pennsylvania

Previous studies with ^{201}Tl and ^{99m}Tc-sestamibi (MIBI) have used large field of view (LFOV) cameras not optimized for breast imaging. The purpose of this study was to compare these agents and to determine if a small field of view (SFOV) camera designed to minimize the camera-to-breast distance could improve tumor detection. **Methods:** A 28-cm (SFOV) camera was fitted with slant-hole and diverging collimators to perform craniocaudal scintigraphy for direct comparison with mammography. Of the 46 patients studied, 20 had ^{201}Tl imaging alone and 26 had combined ^{201}Tl and MIBI imaging. LFOV (40 cm) breast and axillary images also were obtained. Visual and quantitative analyses of tumor uptake were performed. **Results:** The SFOV camera with nonparallel collimation showed variable ^{201}Tl and MIBI normal breast activity. This was partly due to significant scatter from cardiac and abdominal activity. Overall, ^{201}Tl had a sensitivity of 53%, which was 67% for tumors ≥1.5 cm and 20% for tumors ≤1.5 cm. MIBI sensitivity was 90% (9/10) for lesions ≥ 1.5 cm. Specificity was 93% for ^{201}Tl and 83% for MIBI. There was no significant difference in ^{201}Tl (1.76 ± 0.55) and MIBI (1.82 ± 0.95) tumor uptake ratios (p = 0.75). **Conclusion:** Technetium-99m-MIBI was more sensitive than ^{201}Tl for imaging lesions ≥1.5 cm. Craniocaudal positioning minimized the camera-to-breast distance but did not increase ^{201}Tl detection of tumors <1.5 cm and increased background breast activity due to scatter.

Key Words: thallium-201; technetium-99m-sestamibi; breast cancer; mammoscintigraphy; tumor detection

J Nucl Med 1995; 36:1696–1700

Breast cancer continues to be a leading cause of death in women in the United States. Mammography has been accepted as the primary screening test for breast cancer because of its low cost and high sensitivity for detecting small lesions (<1 cm), even when they are clinically nonpalpable. It cannot, however, always be used to differentiate benign from malignant lesions accurately and has a low positive predictive value, ranging from 15% to 30% (*1*). Because mammography is not always specific, biopsies are frequently performed for what prove to be benign lesions.

Both ^{201}Tl and ^{99m}Tc-sestamibi (MIBI) are useful tumor imaging agents. Early studies of ^{201}Tl (*2–4*), and more recently of MIBI (*5–8*), have shown that these agents are frequently taken up by breast cancers. These previous studies, however, used large field of view (LFOV) cameras not optimized for breast imaging and reported positive results primarily on large, palpable lesions greater than 1.5 cm.

The purpose of this study was to investigate whether a conventional gamma camera optimized for imaging small organs such as the breast could improve scintigraphic breast tumor detection, especially of lesions less than 1.5 cm. Initially, this study was begun using ^{201}Tl only and later modified to include a direct comparison of ^{201}Tl and MIBI.

METHODS

Forty-six women (aged 42–81 yr) with a breast lesion and correlative mammograms who were to undergo either fine needle aspiration or surgical excision biopsy were studied. The study protocol was approved by the Temple University Institutional Review Board. All patients gave informed consent.

A small field of view (SFOV), 28-cm diameter gamma camera was fitted with both 30° slant-hole and diverging collimators to minimize the camera-to-breast distance. Extrinsic camera resolution for these collimators and a standard parallel-hole collimator were compared using FWHM measurements.

The first 20 patients received a single intravenous injection of 74 MBq ^{201}Tl. Images were acquired 20 min postinjection using a 128 × 128 matrix over the 71-KeV photopeak of ^{201}Tl with a 20% window and craniocaudal orientation to permit direct comparison to the mammogram (Fig. 1). A standard radiologic lead apron was drapped over the imaging table and below the patient to reduce scattered counts from the abdomen.

Each breast was imaged for either 100K cts or 5 min. If the breast lesion was palpable, an image with a marker on the lesion was also obtained in the same projection. After imaging with the SFOV camera, anterior, right and left anterior oblique axillary images were also acquired for 500K cts using a 128 × 128 matrix and a large field of view (LFOV) (40 cm) camera.

After the first 20 patients were imaged, the study was modified to include a comparison of ^{201}Tl and MIBI images. The remaining 26 patients were injected with ^{201}Tl (74 MBq) and images were acquired according to the sequence previously described. Upon

Received Jul. 19, 1994; revision accepted Jan. 12, 1995.

For correspondence or reprints contact: Alan H. Maurer, MD, Director, Nuclear Medicine, Temple University Hospital, Broad and Ontario Strs., Philadelphia, PA 19140.

FIGURE 1. Camera-collimator positioning for craniocaudal breast imaging. Each breast is imaged individually with the camera above and the breast positioned on a lead-lined support to reduce scatter from below.

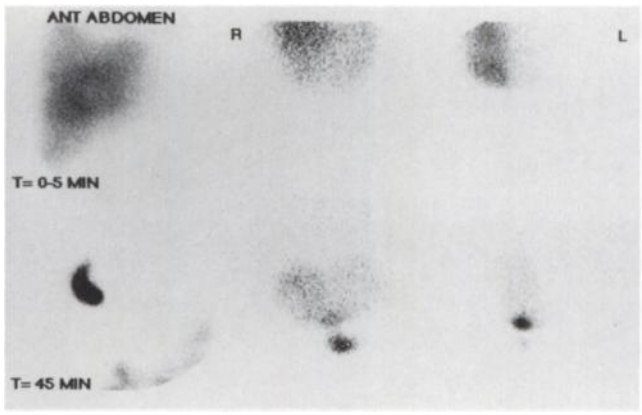

FIGURE 2. (Top) Anterior image of the liver obtained with the same diverging collimator used for breast imaging. Both right (R) and left (L) craniocaudal breast images were acquired before disofenin excretion into the bowel or concentration in the gallbladder. The medial portion of each breast is at the center and the lateral aspect is located on the right (R) and left (L). Nonuniform background activity primarily from scattered counts from the liver is seen throughout the right breast, primarily along the medial aspect of the left breast. (Bottom) After visualization of the gallbladder, focal hepatic activity is seen outside the area of the right breast but appears within the left breast.

completion of ^{201}Tl imaging, 555 MBq MIBI were administered intravenously and 100K craniocaudal breast images using the 140-KeV photopeak and a 20% window were obtained beginning 1–2 min postinjection and then every 20 min for up to 3 hr. An anterior image of the chest as well as right and left anterior oblique axillary 500K cts images were also acquired using a 128 × 128 matrix and the LFOV camera 20 min after the MIBI injection.

For visual analysis, two observers reviewed the images with knowledge of the lesion location on the craniocaudal mammograms. Lesion determinations as ^{201}Tl- (or MIBI-positive or negative were made by consensus). A lesion was visually positive if there was focal uptake of the radiopharmaceutical in the area of the known mammographic lesion greater than the immediately adjacent normal breast tissue.

If visually positive, a quantitative uptake ratio was calculated by placing a manual ROI on the area of the lesion in the initial set of ^{201}Tl and MIBI images. The ^{201}Tl ratios were therefore obtained approximately 20 min postinjection and the MIBI ratios 5 min postinjection. An uptake ratio for each visualized tumor was calculated as the ratio of the mean counts per pixel in the tumor region of interest (ROI) divided by the mean counts per pixel in a normal background ROI. All comparisons (tumor-to-background) were made using the paired t-test.

To evaluate the effect of scattered counts from high levels of hepatic and abdominal activity, we studied two patients who had hepatobiliary studies for suspected gallbladder disease who consented to have breast imaging. With the SFOV camera and diverging collimator, an anterior image of the liver was obtained for 2 min beginning 2–3 min after injection of 5 mCi ^{99m}Tc-disofenin. Immediately after this injection, right and left craniocaudal breast images were acquired for 2 min (Fig. 2). Regions of interest were placed over the right and left breast images to obtain the total counts in each breast as a percentage of the total liver counts. In addition, delayed images of each breast were acquired following visualization of the gallbladder and intestinal activity.

RESULTS

The FWHM measurements for the three camera-collimator combinations were similar: parallel-hole = 6.0 mm, slant-hole = 6.0 mm and diverging = 6.5 mm. After studying the first five patients, the diverging collimator was judged to be optimal for positioning, especially for small breasts, and to include lesions near the chest wall. It was then used exclusively for the remainder of the study.

Biopsies were performed on 48 breast lesions; the clinical results were 31 benign lesions, including 5 papillomas, 11 fibroadenomas and 15 fibrocystic lesions. Thallium-201 was negative in 28 of 30 benign lesions for a specificity of 93%. The false-positive ^{201}Tl lesions included one cellular fibroadenoma and one papilloma. Technetium-99m-MIBI was negative in 15 of 18 benign lesions for a specificity of 83%. MIBI-positive lesions included two benign papillomas and one fibroadenoma.

The malignant lesions (n = 17) included: ductal (n = 14), medullary (n = 2) and lobular (n = 1) carcinomas. The results for positive visual identification of these lesions by size are shown in Table 1. The overall sensitivity for ^{201}Tl was 53% (9/17). For lesions greater than 1.5 cm the sensitivity was 67% (8/12) and 20% (1/5) for lesions smaller than 1.5 cm. The sensitivity for MIBI was 90% (9/10) for lesions greater than 1.5 cm. Only one patient with a lesion less than 1.5 cm was studied with ^{201}Tl and MIBI.

Ten axillary lymph node dissections were performed. Of these, four patients had surgically positive nodes. Only one patient (imaged with ^{201}Tl alone) had a positive study, with uptake in a palpable 2 × 2-cm axillary lymph node.

TABLE 1
Visualization of Tumors by Size

Size	Tl(+)	Tl(−)	MIBI(+)	MIBI(−)
<1 cm	1	2	1	
1–1.4 cm		2		
1.5–2.0 cm	3	1	4	
>2 cm	5	3	5	2

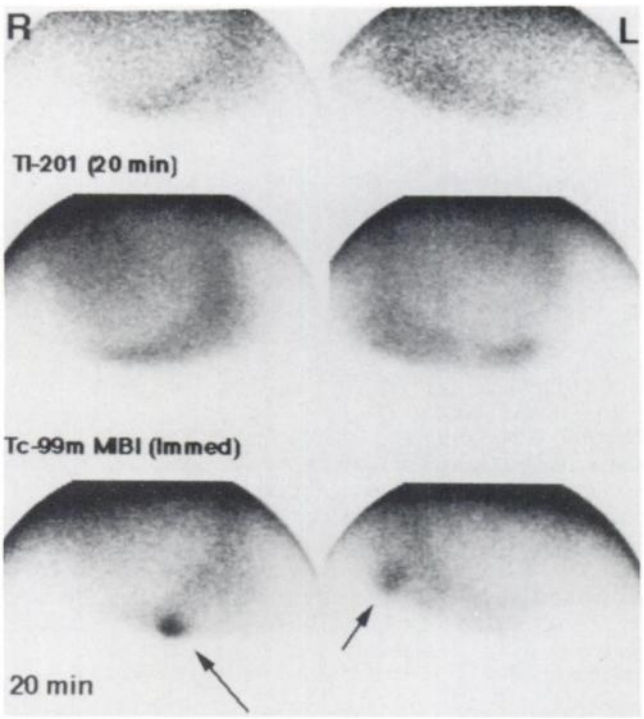

FIGURE 3. Comparison of normal ^{201}Tl and MIBI breast images. All views are shown with the camera positioned above each breast as in Figures 1 and 2. The medial portion of each breast is at the center and the lateral aspect is located on the right (R) and left (L). (Top) Normal ^{201}Tl images show symmetrical nonuniform activity in each breast. (Middle) Immediate (1–2 min) postinjection MIBI images show similar uptake in each breast. (Bottom) As early as 20 min postinjection, focal localization of MIBI is seen in both the right and left breast (arrows), probably due to gallbladder activity as seen in Figure 2.

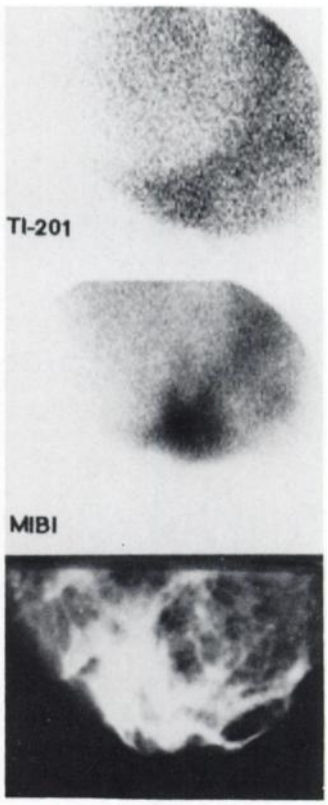

FIGURE 4. Correlation of ^{201}Tl and MIBI breast activity in dense fibroglandular breast tissue. (Top) Twenty-minute ^{201}Tl image shows increased activity which correlates with the dense breast tissue on the mammogram (Bottom). (Middle) Initial MIBI breast image shows similar activity correlating with the location of dense fibroglandular tissue.

Craniocaudal ^{201}Tl and MIBI images obtained with the SFOV camera and diverging collimator demonstrated nonuniform activity in normal breast tissue (Fig. 3). This nonuniform uptake was not seen in the LFOV images and was likely due in part to a significant amount of scattered counts from the liver. In spite of the contribution from scattered counts, focal ^{201}Tl and MIBI uptake in normal breast tissue did appear to correlate anatomically with the location of dense fibroglandular tissue (Fig. 4) in some patients.

In the two patients with suspected gallbladder disease, the scatter contribution of liver counts to the right breast was higher than the left, with a range of 20%–36% (mean = 28%). The mean activity on the left was 18% (range 12%–25%), with visible localization to the medial portion of the left breast (Fig. 2). After disofenin localization in the gallbladder, focal activity due to scatter was seen both outside and within the breast (Fig. 2), which explains the focal activity occasionally seen in some MIBI studies 20 min postinjection (Figs. 3, 5). Scattered counts from the heart also were visible in some of the ^{201}Tl and MIBI breast images (Fig. 5). In general, the amount of scatter in the breast was dependent on the degree of caudal angulation of the camera head needed to obtain optimum breast positioning.

For those patients imaged with both MIBI and ^{201}Tl, there was congruency in tumor positivity. Thallium-201 and MIBI were positive in seven tumors, with two false-negatives. Visually, tumor uptake of MIBI appeared consistently higher than ^{201}Tl (Figs. 6, 7). While the uptake ratios tended to be higher for MIBI (mean = 1.82 ± 0.95) than ^{201}Tl (1.76 ± 0.55), they were not statistically significant ($p = 0.75$), probably because of the higher MIBI background.

DISCUSSION

Numerous studies have found that both ^{201}Tl and MIBI have a high negative predictive value (>90%) for evaluating large breast lesions prior to biopsy (*2–8*). The results from these investigations indicate that a negative study in a patient with a large breast mass might preclude the need for biopsy. We sought to determine if such an approach would be valid for small mammographic lesions (<1.5 cm) if we could reliably image these lesions with a dedicated SFOV camera.

Of the camera-collimator systems tested, we found the diverging collimator and SFOV camera to be optimal for positioning the breast in the craniocaudal projection. This view was chosen because it facilitates direct comparison to mammography. Our ability to position the diverging collimator directly on the breast helped to increase resolution, admittedly at the expense of higher scatter. In two patients, we found as much as 25%–30% of liver counts contributing as scatter in the breast. This scatter contribution, however, would vary from patient to patient depending on breast size, body habitus, liver uptake and the angulation of the

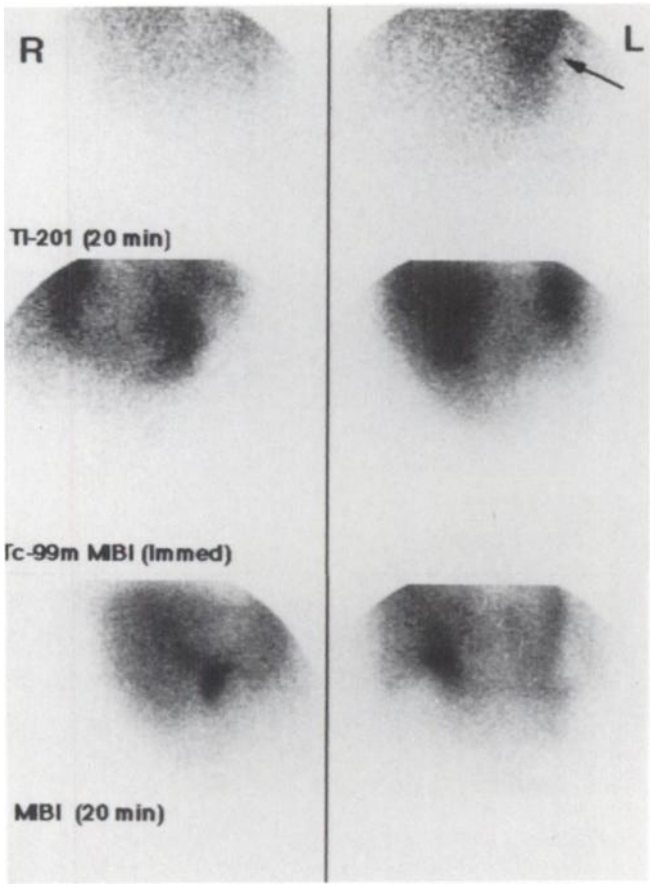

FIGURE 5. Comparison of ^{201}Tl and MIBI images in normal breast tissue. (Top) Thallium-201 images show minimal background with scatter (arrow) from the heart seen near the chest wall. (Middle) Initial MIBI images show more intense background in normal breast tissue, probably due to higher hepatic uptake. (Bottom) Focal localization of MIBI is seen in both breasts 20 min postinjection, probably due to gallbladder activity as demonstrated in Figure 2.

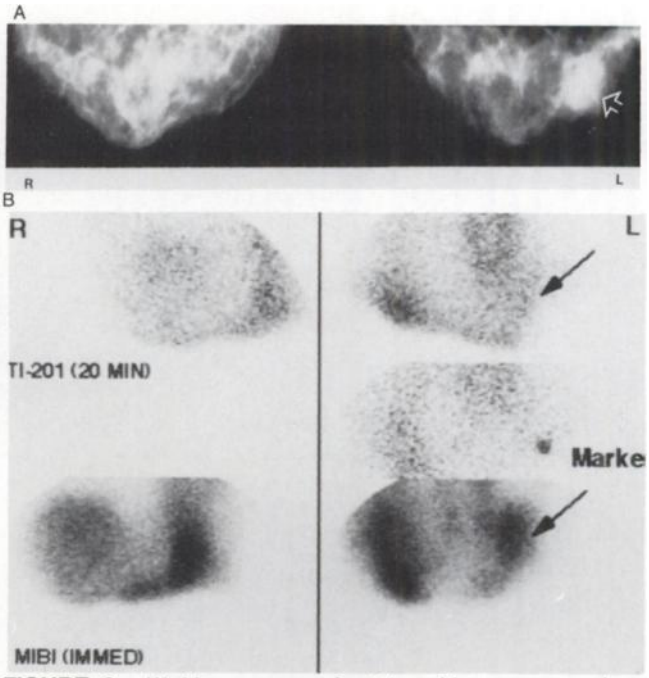

FIGURE 6. (A) Mammogram of a 51-yr-old woman reveals a 2-cm left infiltrating ductile carcinoma (open arrow). (B) Top row. Thallium-201 images, while positive, show minimal tumor activity (upper arrow) (ratio = 1.4) compared with more prominent (bottom row) MIBI uptake in the tumor (ratio = 1.6) Note that the ^{99m}Tc-MIBI uptake ratio is lowered by the higher background activity.

camera head. We anticipate that changes in collimator design and the imaging table will help to reduce this scatter.

We did find ^{201}Tl and ^{99m}Tc-MIBI uptake in normal breast tissue that did not correspond to the expected pattern of scatter from the liver or heart (Fig. 3). In addition, focal uptake often appeared increased in areas of dense fibroglandular breast tissue (Fig. 4). Lee et al. hypothesized that "normal glandular breast tissue is not thallium-avid." This has been proposed as one of the advantages of ^{201}Tl imaging, especially for scintigraphy of younger patients with dense glandular tissue (*4*). Our results indicate that high-resolution images of the breast with either ^{201}Tl or MIBI may show some normal glandular activity.

We had hoped that our ability to position the collimator directly on the breast would significantly increase resolution and detection rates of small lesions. Our initial protocol included only ^{201}Tl imaging. After imaging our group of 20 patients, we found that our camera-collimator system did not increase our ability to detect lesions smaller than 1.5 cm (*9*). This was probably due in part to the increased background of normal breast tissue, especially for right-sided lesions. We observed no increase in sensitivity in the left breast, where the background scatter contribution was less. This limitation of ^{201}Tl scintigraphy to detect tumors less than 1.5 cm is similar to the results of others for thyroid and lung carcinomas even with SPECT (*10,11*).

Other studies have attempted to use SPECT for MIBI breast tumor imaging. Villanueva-Meyer et al. (*7*) found the smallest lesion detected was 0.8 cm but only 5/9 (56%) larger tumors (2–5 cm) had a positive study. Nagaraj et al. (*9*) reported a sensitivity and specificity for planar imaging of 80% and 70%, respectively, whereas these values were 87% and 50% for SPECT. In the series by Nathan et al. (*10*), planar imaging detected 8 of 18 lesions and SPECT detected 10 of 18 lesions. The eight negative lesions detected by SPECT were 1 cm or smaller.

We included MIBI in our protocol not only to compare it directly with ^{201}Tl in the same patients but also to see if a ^{99m}Tc agent could improve small lesion detection. Although the overall detection rate for large lesions (>1.5 cm) was higher for MIBI (90%) than ^{201}Tl, we cannot make any definite conclusions on MIBI's ability to detect lesions under 1.5 cm because only one tumor less than 1.5 cm was studied with MIBI.

Our series included only a small number of patients with positive axillary node dissections. Neither ^{201}Tl nor MIBI were sensitive for detecting lymph node involvement (3/4 negative), but our sample size was small (four patients) and we cannot make any definite conclusions on the sensitivity of ^{201}Tl or MIBI for detecting axillary disease.

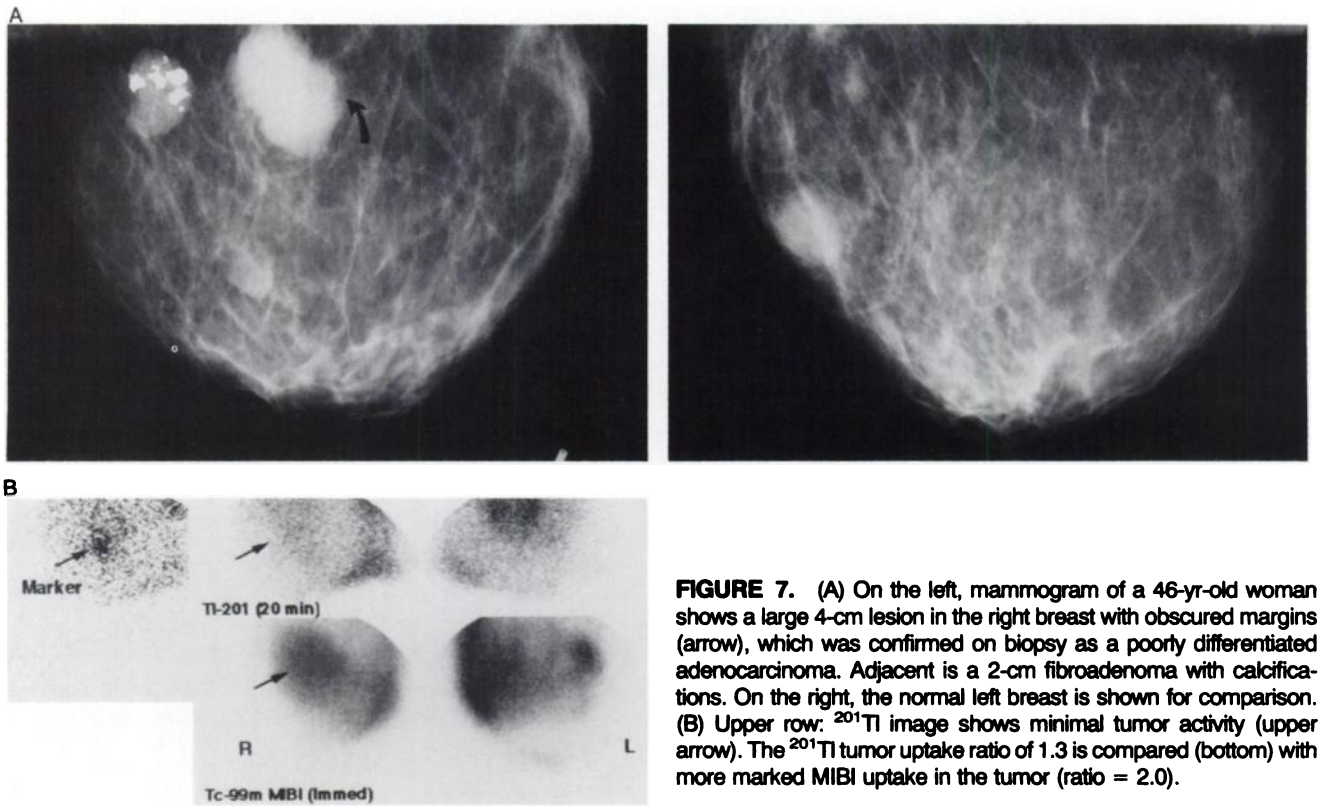

FIGURE 7. (A) On the left, mammogram of a 46-yr-old woman shows a large 4-cm lesion in the right breast with obscured margins (arrow), which was confirmed on biopsy as a poorly differentiated adenocarcinoma. Adjacent is a 2-cm fibroadenoma with calcifications. On the right, the normal left breast is shown for comparison. (B) Upper row: ^{201}Tl image shows minimal tumor activity (upper arrow). The ^{201}Tl tumor uptake ratio of 1.3 is compared (bottom) with more marked MIBI uptake in the tumor (ratio = 2.0).

CONCLUSION

Ultimately the ability to image small breast cancers scintigraphically will require radiopharmaceuticals with high tumor-to-background ratios used in conjunction with high-resolution cameras. Because many small breast lesions as well as lesions close to the chest wall cannot be easily imaged with LFOV planar or SPECT cameras, imaging devices for mammoscintigraphy will need additional optimization. Recent reports with MIBI and prone imaging report high specificity and sensitivity for breast cancers (*11–13*). Because of the ease of craniocaudal positioning and the ability to minimize the camera-to-breast distance with the SFOV camera, we are pursuing modifications to our approach that will hopefully reduce the scatter and nonspecific breast activity seen in this study. In the future, planar techniques that combine the advantages of both prone and craniocaudal imaging may yield the most favorable results.

ACKNOWLEDGMENTS

The authors thank Leslie Boshko, Kelly Wharton and Vince Cherico for their technical assistance and Milne Hewis for photographic work. Financial support provided by DuPont Merck Pharmaceutical Company, Radiopharmaceutical Division, N. Billerica, MA.

REFERENCES

1. Kopans DB. The positive predictive value of mammography. *AJR* 1992; 158:521–526.
2. Sehweil AM, McKillop JH, Milroy R, et al. Thallium-201 scintigraphy in the staging of lung cancer, breast cancer and lymphoma. *Nucl Med Commun* 1990;11:263–269.
3. Waxman AD, Ramanna L, Memsic LD, et al. Thallium scintigraphy in the evaluation of mass abnormalities of the breast. *J Nucl Med* 1993;34:18–23.
4. Lee VW, Sax EJ, McAneny DB, et al. A complementary role for thallium-201 scintigraphy with mammography in the diagnosis of breast cancer. *J Nucl Med* 1993;34:2095–2100.
5. Khalkhali I, Cutrone J, Mena I, Diggles L, Venegas R, Vargas H. Clinical and pathologic follow-up of 100 patients with breast lesions studied with scintimammography [Abstract]. *J Nucl Med* 1994;35(suppl):22P.
6. Lastoria S, Varrella P, Mainolfi C, et al. Technetium-99m-sestamibi scintigraphy in the diagnosis of primary breast cancer [Abstract]. *J Nucl Med* 1994;35(suppl):22P.
7. Villanueva-Meyer J, Leonard Jr MHL, Ali S, Cesani F, Kumar D. Technetium-99m sestamibi in the evaluation of mammographic abnormalities [Abstract]. *J Nucl Med* 1994;35(suppl):229P.
8. Waxman A, Nagaraj N, Ashok G, et al. Sensitivity and specificity of Tc-99m methoxy isobutal isonitrile (MIBI) in the evaluation of primary carcinoma of the breast: comparison of palpable and nonpalpable lesions with mammography [Abstract]. *J Nucl Med* 1994;35(suppl):22P.
9. Nagaraj N, Waxman A, Ashok G, et al. Comparison of SPECT and planar Tc-99m sestamibi (MIBI) imaging in patients with carcinoma of the breast [Abstract]. *J Nucl Med* 1994;35:229P.
10. Nathan MA, Seabold JE, Barloon T, et al. Planar versus SPECT MIBI evaluation of suspicious breast lesions on mammography: histologic correlation [Abstract]. *J Nucl Med* 1994;35(suppl):229P.
11. Jochelson MS, Waxman A, Nagaraj N, Phillips E, Yadegar J. Technetium-99m methoxy isobutyl isonitril breast imaging in conjunction with mammography: review of 350 cases [Abstract]. *Radiology* 1994;193(P):158.
12. Khalkhali I, Cutrone JA, Mena IG, Diggles LE, Klein SR. Scintimammography versus mammography: complimentary role of Tc-99m sestamibi breast imaging in the prone position for the diagnosis of breast carcinoma [Abstract]. *Radiology* 1994;193(P):158.
13. Khalkhali I, Mena I, Jouranne E, et al. Prone scintimammography in patients with suspicion of carcinoma of the breast. *J Am Coll Surg* 1994;78: 491–497.